SHEP-08-21
November 28, 2008

One-loop Electro-Weak Corrections to Three-jet Observables of b-quarks in e^+e^- Annihilations[1]

C.M. Carloni-Calame[1], S. Moretti[1], F. Piccinini[2] and D.A. Ross[1]

[1] *School of Physics and Astronomy, University of Southampton Highfield, Southampton SO17 1BJ, UK*

[2] *INFN - Sezione di Pavia, Via Bassi 6, 27100 Pavia, Italy*

Abstract

We compute the full one-loop EW contributions of $\mathcal{O}(\alpha_{\rm S}\alpha_{\rm EM}^3)$ entering the electron-positron into two b-quarks and one gluon cross section at the Z peak and LC energies. We include both factorisable and non-factorisable virtual corrections, photon bremsstrahlung but not the real emission of $W^\pm$ and Z bosons. Their importance for the measurement of $\alpha_{\rm S}$ from jet rates and shape variables is explained qualitatively and illustrated quantitatively. Their impact on the forward-backward asymmetry is also analysed.

1 Introduction

Jet samples enriched in b-quarks produced in e^+e^- annihilations are used for sophisticated tests of QCD, primarily because they enable one to distinguish between quarks and gluons, thanks to b-flavour tagging (typically, by exploiting high p_T leptons and/or microvertex techniques). This is unlike the case of lighter flavours[2]. To name but a few examples, by studying b-jet samples, one can: (i) verify the flavour independence of $\alpha_{\rm S}$; (ii) study the

[1]Work supported in part by the U.K. Science and Technology Facilities Council (STFC), by the European Union (EU) under contract MRTN-CT-2006-035505 (HEPTOOLS FP6 RTN) and by the Italian Ministero dell'Istruzione, dell'Università e della Ricerca (MIUR) under contract 2006020509_004.

[2]With the possible exception of c-quarks, whose tagging efficiency is however much lower in comparison to that of b-quarks, so as to make the former much less suitable than the latter to phenomenological investigation.

properties of the QCD force carrier (the gluon); (iii) measure the b-quark mass. (For an authoritative review on experimental tests of QCD in e^+e^- events see [1] and references therein.)

Of particular relevance is the three-jet sample, as it impinges on all types of analysis (i)–(iii). It is therefore of paramount importance to give predictions for the $e^+e^- \to b\bar{b}g$ cross section to the highest degree of precision, thereby necessarily involving the computation of all higher order corrections within the Standard Model (SM). Whilst the computation of QCD effects through one-loop has been tackled some time ago [2, 3] the case of Electro-Weak (EW) corrections is not available in the literature. We remedy this shortcoming here, by calculating the full one-loop EW corrections to $b\bar{b}g$ observables in electron-positron annihilations generated via the interference of the graphs in Figs. 1–6 of Ref. [4] (see also [5, 6]) with the tree-level ones for $e^+e^- \to \gamma^*, Z \to \bar{b}bg$. In doing so, notice that we will be including photon bremsstrahlung; in contrast, we will refrain from computing real $W^\pm$ and Z boson radiation, as we will argue that this may not enter the experimental jet samples.

Finally, notice that, while QCD corrections are dominant at low e^+e^- energy, EW ones become relatively more and more important as the latter grows larger, because of surviving Sudakov logarithms from which QCD interactions are immune. Besides, EW corrections also carry the hallmark of parity-violating effects, which are generally peculiar to new physics beyond the SM, so that they ought to be accounted for in its quest.

The plan of the rest of the paper is as follows. In the next Section, we describe the calculation and give the input parameters and jet-selection algorithms. Then, in Sect. 3, we present our numerical results for LEP1/SLC, LEP2 and a future Linear Collider (LC). We conclude in Sect. 4.

2 Calculation

The procedures adopted to carry out our computation have been described in [4], to which we refer the reader for the most technical details. Here, we would only like to point out that we have neglected the masses of the b-quarks throughout. However, whenever there is a $W^\pm$ boson in the virtual loops, account has to be taken of the mass of the top (anti)quark, which we have done. Furthermore, before proceeding to show our results, we should mention the numerical parameters used for our simulations. We have taken the top (anti)quark to have a mass $m_t = 171.6$ GeV. The Z mass used was $M_Z = 91.18$ GeV and was related to the $W^\pm$ mass, M_W, via the SM formula $M_W = M_Z \cos\theta_W$, where $\sin^2\theta_W = 0.222478$. The Z width was $\Gamma_Z = 2.5$ GeV. Also notice that, where relevant, Higgs contributions were included with $M_H = 115$ GeV. For the strong coupling constant, $\alpha_{\rm S}$, we have used the two-loop expression with $\Lambda_{\rm QCD}^{(n_f=4)} = 0.325$ GeV in the $\overline{\rm MS}$ scheme, yielding $\alpha_{\rm S}^{\overline{\rm MS}}(M_Z^2) = 0.118$.

As for the jet definition, partonic momenta are clustered into jets according to the Cambridge jet algorithm [7] (e.g., when $y_{ij} < y_{cut}$ with $y_{cut} = 0.001$), the jets are required to lie in the central detector region $30^\circ < \theta_{\rm jets} < 150^\circ$ and we request that the invariant mass of the jet system $M_{b\bar{b}g}$ is larger than $0.75 \times \sqrt{s}$. If a real photon is present in the final state, it is clustered according to the same algorithm, but we require that at least three "hadronic" jets are left at the end (i.e., events in which the photon is resolved are rejected)[3]. We further make the assumption that both b-jets can be tagged (as described), including their charge (e.g., via the emerging lepton or the jet-charge method). (For sake of illustration we take the efficiency to be one.) In order to show the behaviour of the EW corrections we are calculating, other than scanning in the collider energy, we have considered here the three discrete values of $\sqrt{s} = M_Z$ (also in view of a GigaZ option of a future LC), $\sqrt{s} = 350$ (the $t\bar{t}$ threshold) GeV and $\sqrt{s} = 1$ TeV (as representative of the Sudakov regime).

3 Numerical Results

In Fig. 1, we present the effects on the cross section (integrated within the experimental cuts defined in the previous Section) induced by different terms of the order $\alpha_{\rm S}\alpha^3_{\rm EM}$ contribution relative to the lowest-order cross section for $e^+e^- \to b\bar{b}g$, plotted as a function of the Centre-of-Mass (CM) energy, in the range from 150 GeV to 1 TeV. The curves represent the effects of the QED (virtual and real) corrections only, the gauge bosons self-energy corrections, the non-factorisable graphs involving four- and five-point functions with WW exchange[4], the weak corrections with the non-factorizing WW graphs removed and the sum of the previous ones. Notice that the total effect is increasingly negative, as $\sqrt{s}$ gets larger, reaching the -13% or so level at 1 TeV. As already stressed in Ref. [4] and visible from the plot here, such a big negative correction is mainly due to the presence of the WW non-factorisable graphs, which develop the aforementioned large Sudakov double logarithms in the very high energy regime. The pattern of the various corrections seen here is not very different from the one seen in Ref. [4] (Fig. 7 therein) with the notable difference that in the case of b-samples one can appreciate the onset of the $t\bar{t}$ virtual threshold, which was instead invisible in the fully flavoured sample of Ref. [4].

The ability to efficiently tag b-quark jets enables one to define observables in $b\bar{b}g$ final states which are not (easily) reconstructable in the case of the full three-jet sample. One

[3] As explained in [4], this serves a twofold purpose. On the one hand, from the experimental viewpoint, a resolved (energetic and isolated) single photon is never treated as a jet. On the other hand, from a theoretical viewpoint, this enables us to remove divergent contributions appearing whenever an unresolved gluon is ejected via an infrared (soft and/or collinear) emission, as we are not computing here $\mathcal{O}(\alpha_{\rm S}\alpha^3_{\rm EM})$ one-loop QCD contributions to $e^+e^- \to b\bar{b}\gamma$.

[4] This is a gauge invariant subset of the complete corrections.

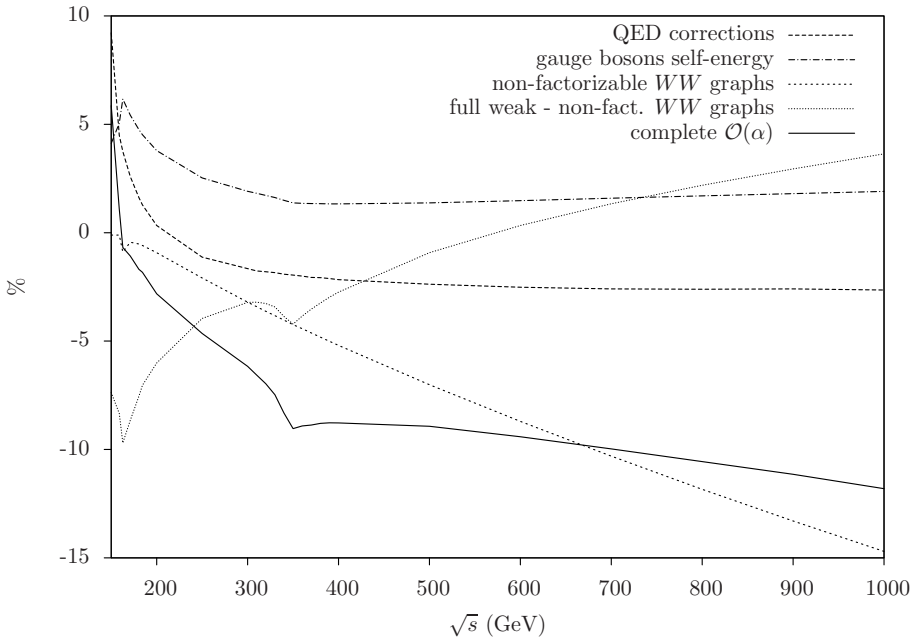

Figure 1: Relative effect on the integrated cross section due to different contributions to the order $\alpha \equiv \alpha_{\rm EM}$ correction, as a function of the CM energy.

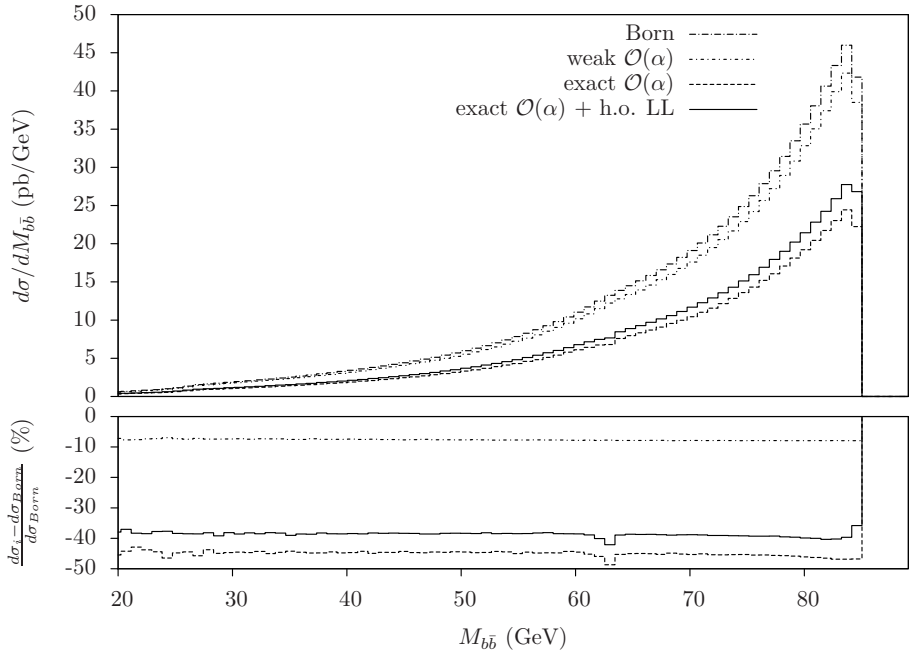

Figure 2: $b\bar{b}$ invariant mass distribution at the Z peak.

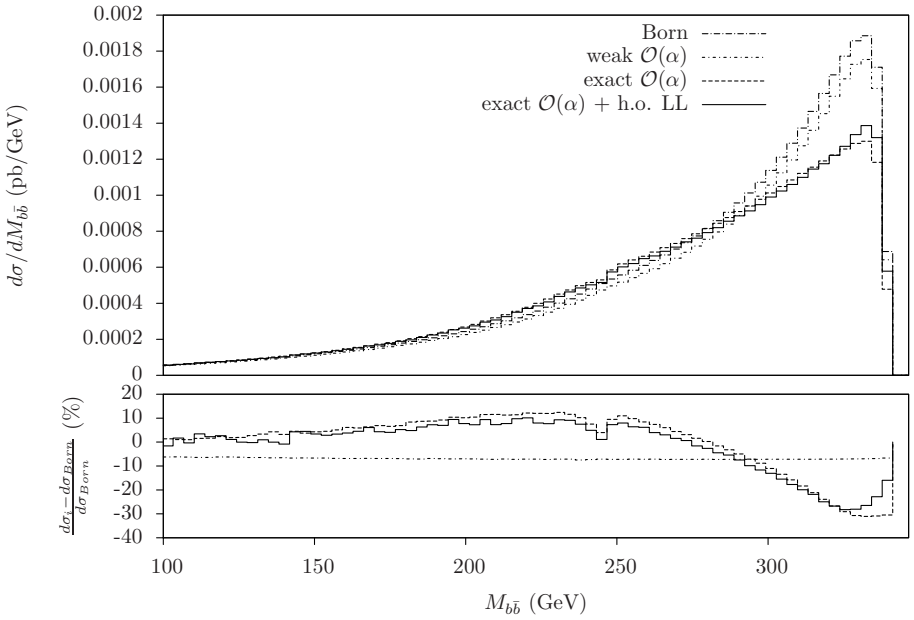

Figure 3: $b\bar{b}$ invariant mass distribution at 350 GeV.

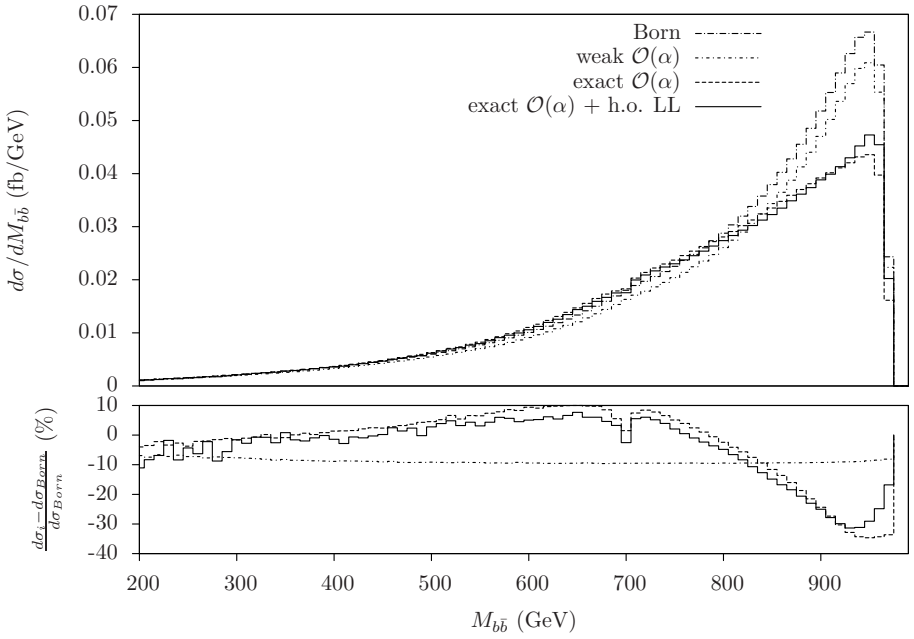

Figure 4: $b\bar{b}$ invariant mass distribution at 1 TeV.

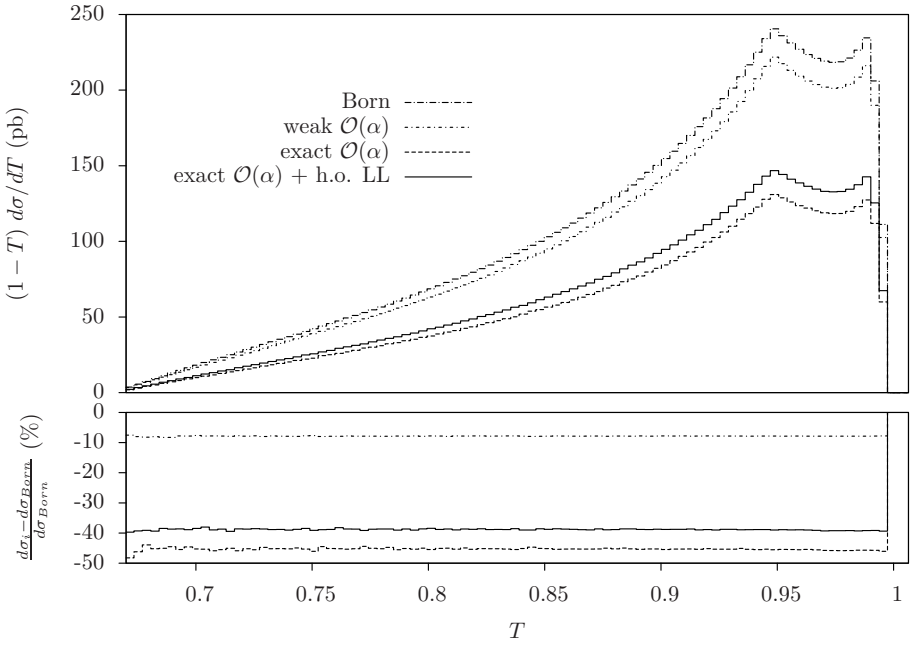

Figure 5: $(1-T)\frac{d\sigma}{dT}$ distribution at the Z peak.

example is the invariant mass of the $b\bar{b}$ pair, $M_{b\bar{b}}$, which we plot in Figs. 2–4. Here, the largest contribution to the total correction comes from QED Initial State Radiation (ISR), primarily because of the radiative return phenomenon.

In fact, the correction is up to 20% for very high energies and intermediate invariant mass and -30% for large invariant mass whereas it is a (constant) -45% at small energy. The purely weak corrections are negative and at the level of -15% at most, for all energies. The higher order QED radiation tends to compensate the order $\alpha_{\rm EM}$ effect, since it enhances the cross section. One should also notice that, again thanks to a Sudakov effect, by raising the CM energy, the relative weight of the weak corrections becomes more important and the effect of higher order QED corrections diminishes. Finally, it is worth noticing that, far from the Z peak, the cut $M_{b\bar{b}g} > 0.75 \times \sqrt{s}$ is more effective in suppressing the radiative return phenomenon, reducing in turn the relative effect of ISR.

In the following some event shape variables are considered[5]: the thrust T [11] and the C-parameter [12] (see Ref. [13] for their definitions). In Figs. 5, 6 and 7, the spectrum of $(1-T)\frac{d\sigma}{dT}$ is shown. This distribution is one of the key observables used for the measurement of $\alpha_{\rm S}$ in e^+e^- collisions [13]. It is worth noticing that whilst the purely weak corrections give an almost constant effect on the whole T range, the presence of the

[5]Recalling footnote 3, one should notice that these observables will depend on y_{cut}. However, this reflects standard experimental procedures [10] aiming at removing resolved photons from the hadronic sample and we also have verified that the relative size of the EW effects computed here does not depend on y_{cut}.

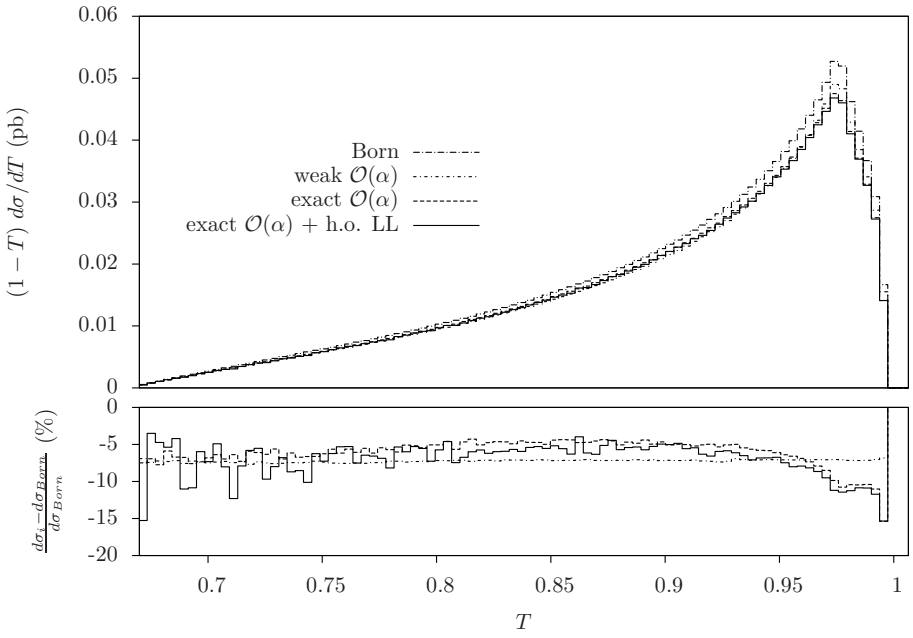

Figure 6: $(1-T)\frac{d\sigma}{dT}$ distribution at 350 GeV.

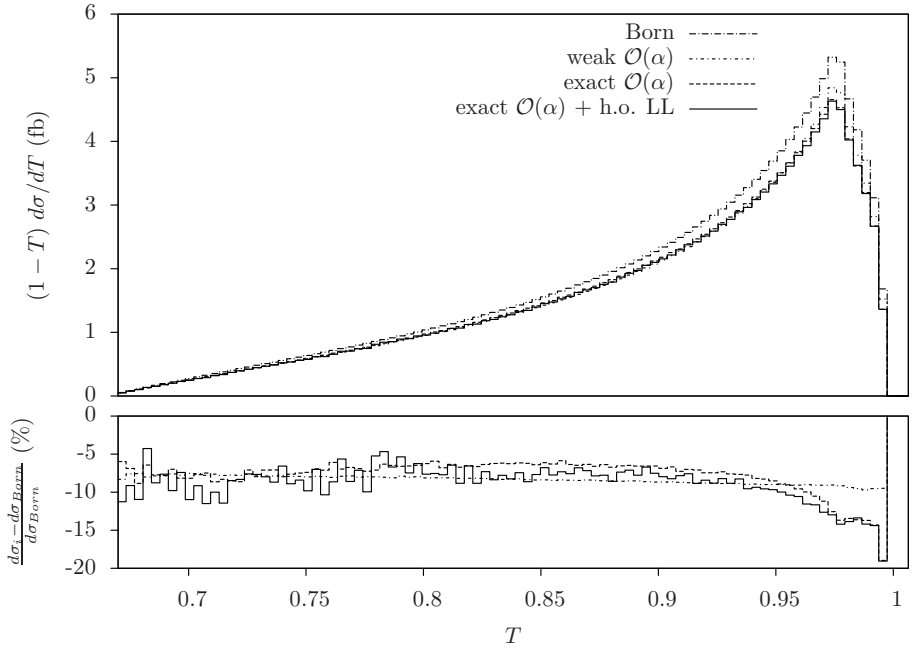

Figure 7: $(1-T)\frac{d\sigma}{dT}$ distribution at 1 TeV.

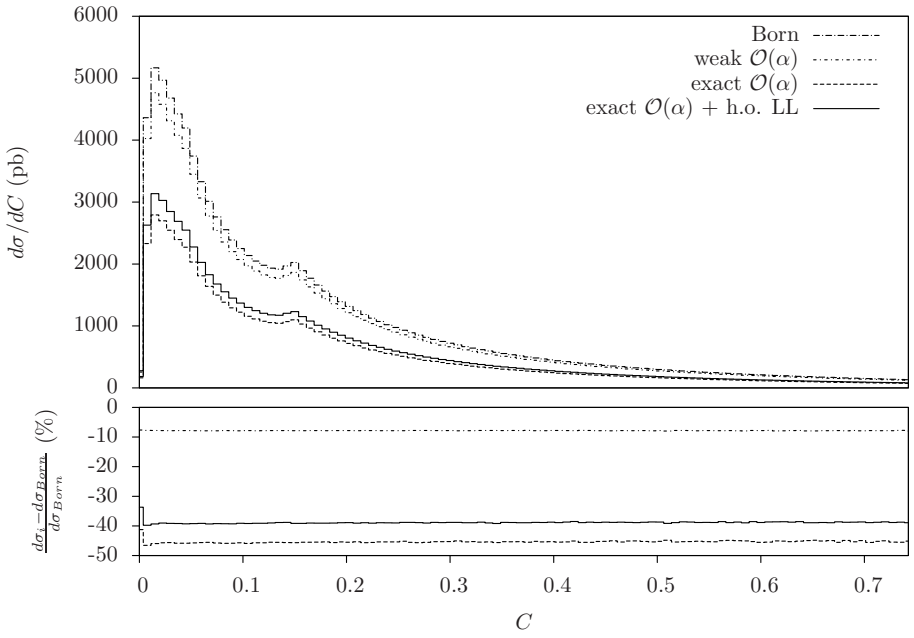

Figure 8: $\frac{d\sigma}{dC}$ distribution at the Z peak.

real bremsstrahlung gives a non-trivial effect in the region $T > 0.95$ (at least at higher energies). The numerical impact of the various contributions is similar in the case of the C-parameter. Here, the region where QED real radiation introduces non-trivial effects is $C \lesssim 0.1$. Given the size of the various EW corrections (the QED ones being of tens of percent), including the purely weak ones (which are steadily at –7% or so) and in view of a precise measurement of $\alpha_{\rm S}$ from $b\bar{b}g$ samples at future LCs, it is clear that such effects will play an important role and thus cannot be neglected.

In Figs. 11, 12 and 13 the Cambridge y distribution is shown. For each event, the observable y is defined as the minimum (Cambridge) y_{ij} such as $y_{ij} > y_{cut} = 0.001$. Also on this distribution the weak effects are quite constant and between –5% and –10% (increasing with energy), while real radiation effects are significantly larger (and negative) and distort the LO shape.

Figs. 14, 15 and 16 present instead the cross sections integrated over y in the range $y_{cut} < y < y_{max}$, as a function of y_{max}. Corrections can be very large in such distributions, generally at any energy, reaching the minus several tens of percent (QED ones) or nearly the –10% (weak ones) level.

If one combines b-(anti)quark flavour tagging with jet-charge measurements, it is possible to define the forward-backward asymmetry, $A_{\rm FB}$, for the case of b-jet samples. As a clear anomaly in this observable (defined already at LO in the case of $b\bar{b}$ final states) has survived after the LEP and SLC era [14, 15], it is worthwhile to investigate the impact that (hitherto neglected) EW contributions through $\mathcal{O}(\alpha_{\rm S}\alpha_{\rm EM}^3)$ can potentially have in

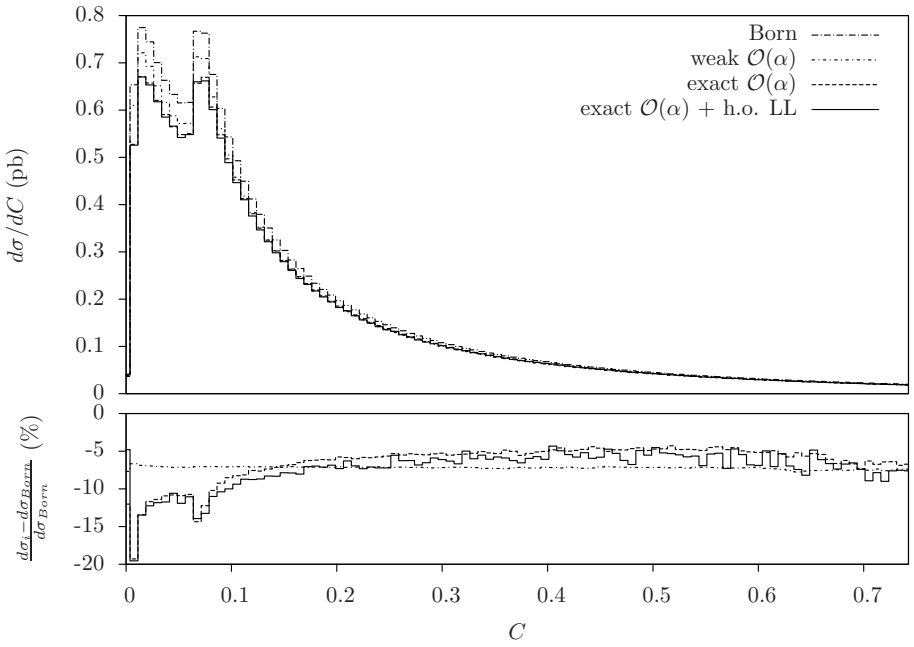

Figure 9: $\frac{d\sigma}{dC}$ distribution at 350 GeV.

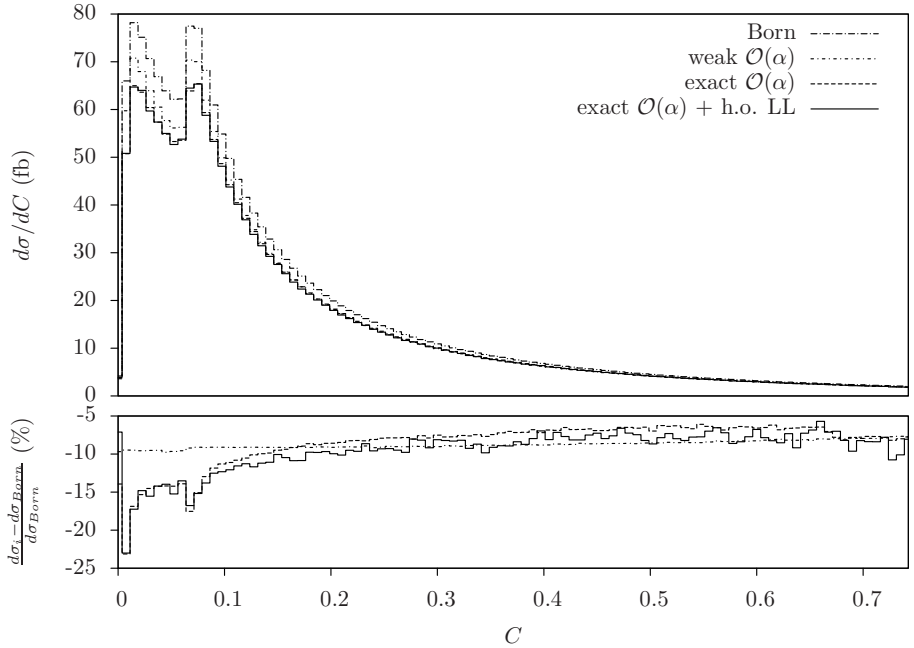

Figure 10: $\frac{d\sigma}{dC}$ distribution at 1 TeV.

addressing the discrepancy between data and SM. Here, we use the following definition for the asymmetry distribution as a function of the $b\bar{b}$ invariant mass:

$$A_{\rm FB}(M_{b\bar{b}}) = \frac{\int_0^{\pi/2} d\theta_b \frac{d\sigma}{d\theta_b dM_{b\bar{b}}} - \int_{\pi/2}^{\pi} d\theta_b \frac{d\sigma}{d\theta_b dM_{b\bar{b}}}}{\int_0^{\pi} d\theta_b \frac{d\sigma}{d\theta_b dM_{b\bar{b}}}} \tag{1}$$

with θ_b being the polar angle of the b-jet relative to the electron, wherein both the numerator and denominator (normalisation) involve only terms of $\mathcal{O}(\alpha_{\rm S}\alpha_{\rm EM}^2)$ plus $\mathcal{O}(\alpha_{\rm S}\alpha_{\rm EM}^3)$ and where the final state comprises three jets. The integrals involved in Eq. (1) are over the phase space allowed by the cuts defined in the previous Section. Whilst the size of the asymmetry is substantial through the computed orders, and the full $\mathcal{O}(\alpha_{\rm S}\alpha_{\rm EM}^3)$ rates are sizeably different from the $\mathcal{O}(\alpha_{\rm S}\alpha_{\rm EM}^2)$ ones (at least at very small and very large energies), our results should clearly be folded with all known higher order corrections to the $e^+e^- \to b\bar{b}$ process (work on this is in progress).

Finally, in Fig. 20, the forward-backward asymmetry, now integrated over $M_{b\bar{b}}$,

$$A_{\rm FB} = \frac{\int_0^{\pi/2} d\theta_b \frac{d\sigma}{d\theta_b} - \int_{\pi/2}^{\pi} d\theta_b \frac{d\sigma}{d\theta_b}}{\int_0^{\pi} d\theta_b \frac{d\sigma}{d\theta_b}} \tag{2}$$

is plotted as a function of the CM energy and as obtained at lowest order and by including only QED corrections or the full one-loop EW corrections. As the CM energy raises, the increasing effect of the purely weak corrections is more and more evident.

4 Conclusions

A careful analysis of actual $e^+e^- \to b\bar{b}g$ data is in order then, involving one-loop EW effects. In this regard though, one *caveat* should be borne in mind: as emphasised in Refs. [8, 9] (albeit in the hadronic context), particular care should be devoted to the treatment of real $W^\pm$ and Z radiation and decay in the definition of the jet sample, as this will determine whether tree-level $W^\pm$ and Z bremsstrahlung effects (neglected here) have to be included in the theoretical predictions through $\mathcal{O}(\alpha_{\rm S}\alpha_{\rm EM}^3)$. However, given the cleanliness of jet samples produced in electron-positron machines, as compared to hadronic ones, we believe that the former contribution can effectively be disentangled, thereby rendering our present predictions of immediate experimental relevance.

Acknowledgements

SM thanks FP for financial support during a visit to Pavia while FP thanks SM and DAR for hospitality in Southampton. CMCC acknowledges partial financial support from the British Council in the form of a 'Researcher Exchange Programme' award and from the Royal Society via a 'Short Visit to the UK' grant.

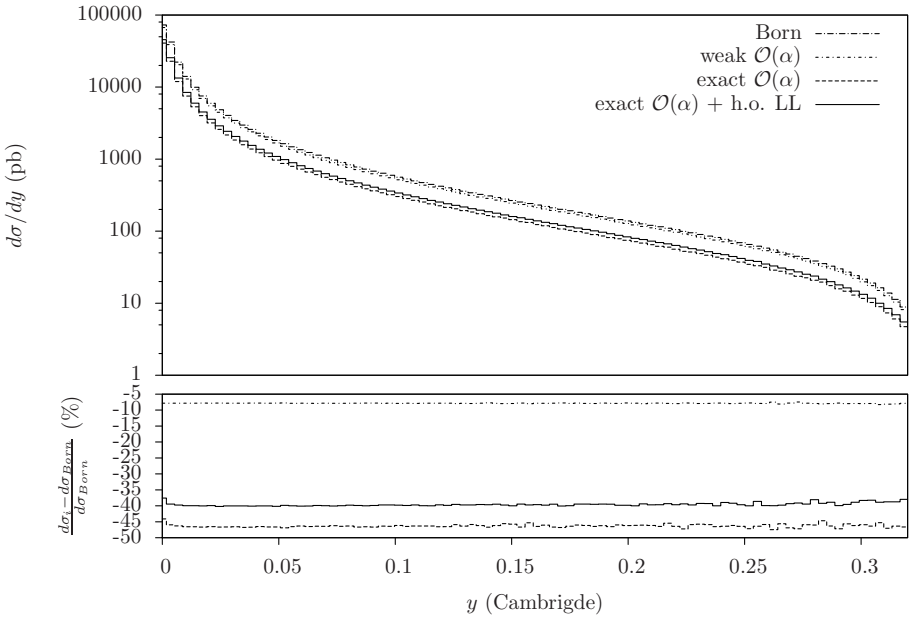

Figure 11: Cambridge y distribution at the Z peak.

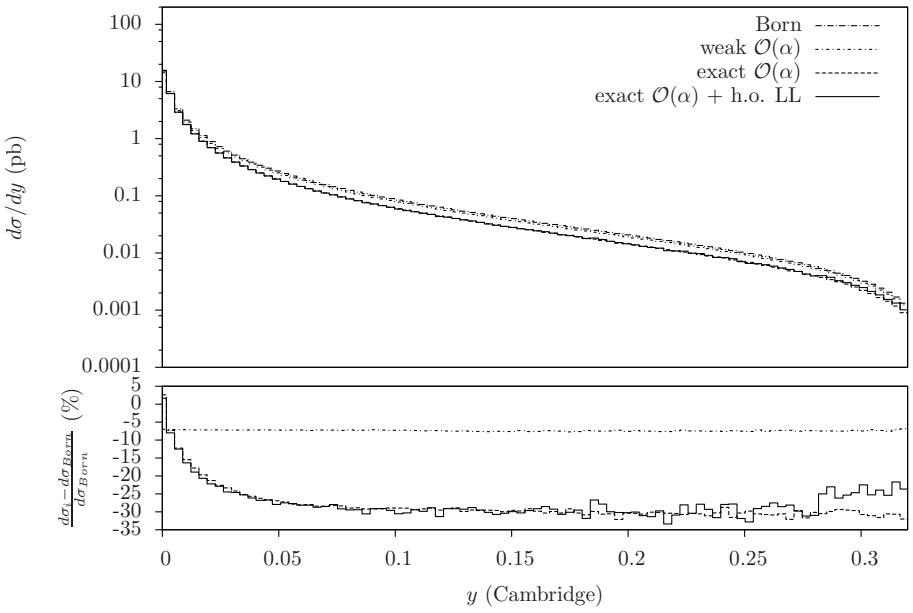

Figure 12: Cambridge y distribution at 350 GeV.

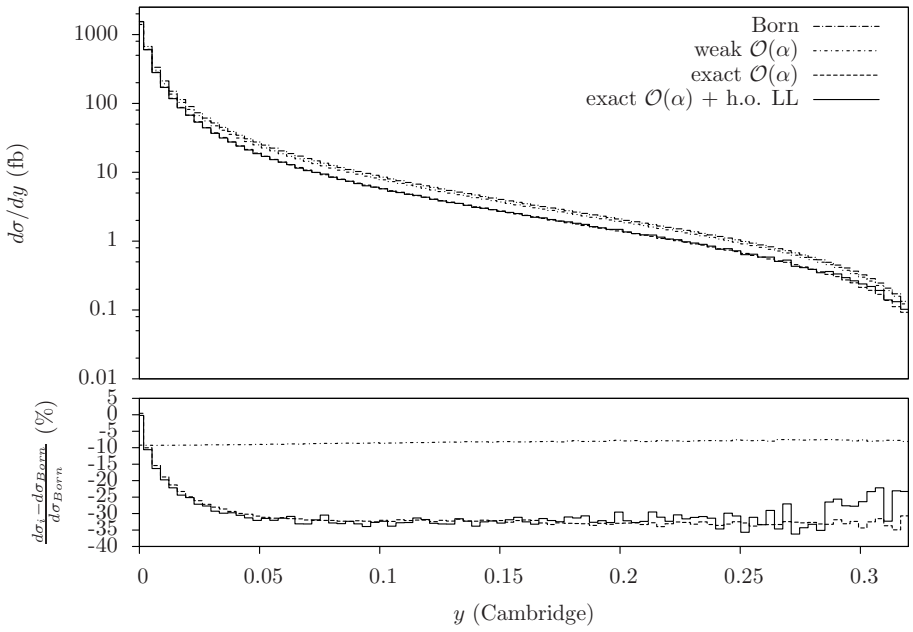

Figure 13: Cambridge y distribution at 1 TeV.

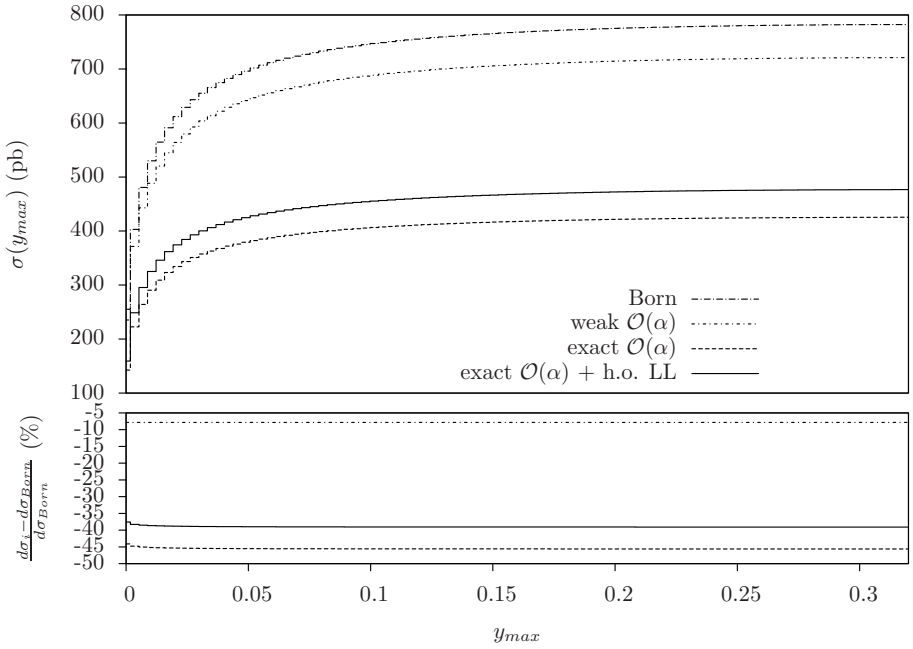

Figure 14: Cross section as a function of the Cambridge maximum y at the Z peak.

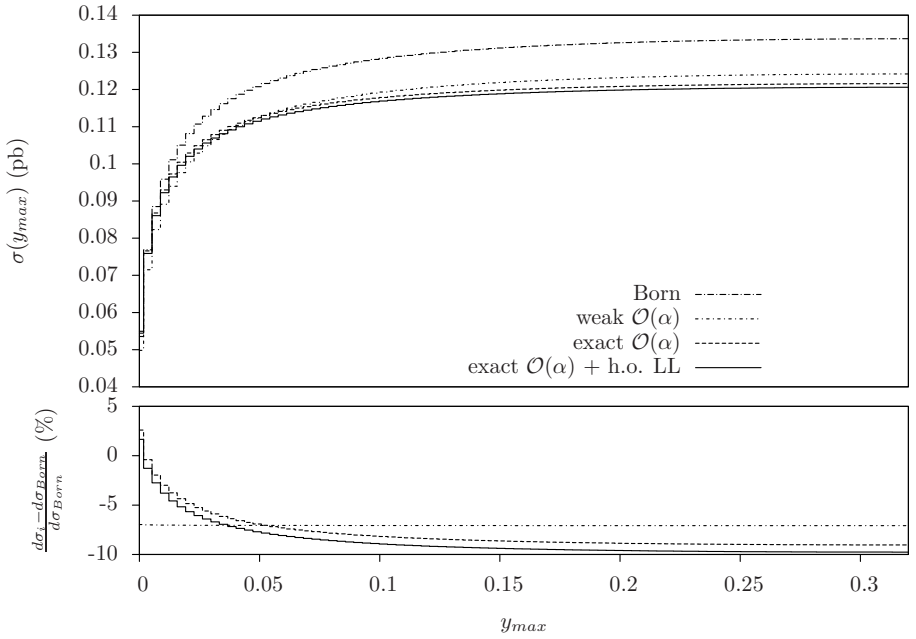

Figure 15: Cross section as a function of the Cambridge maximum y at 350 GeV.

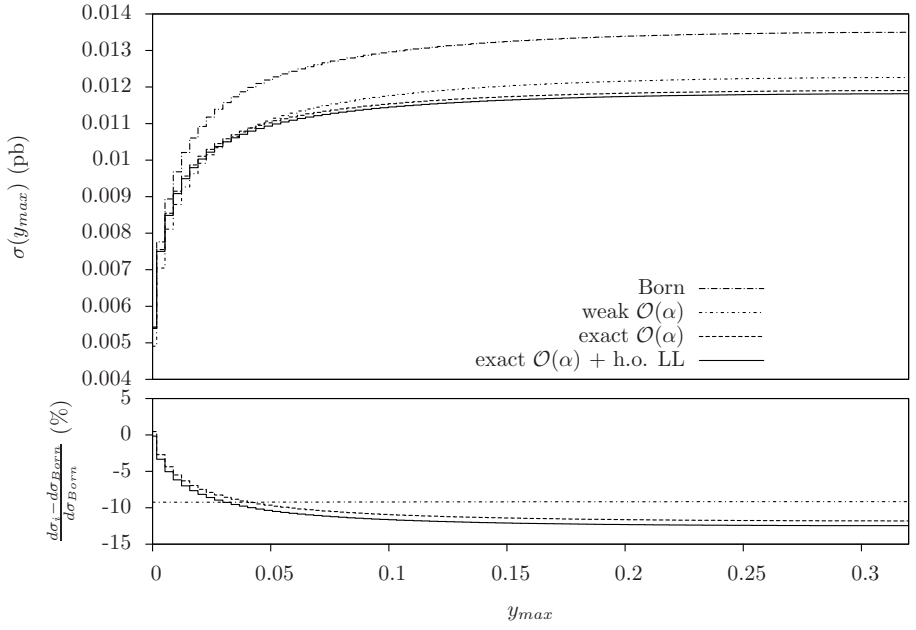

Figure 16: Cross section as a function of the Cambridge maximum y at 1 TeV.

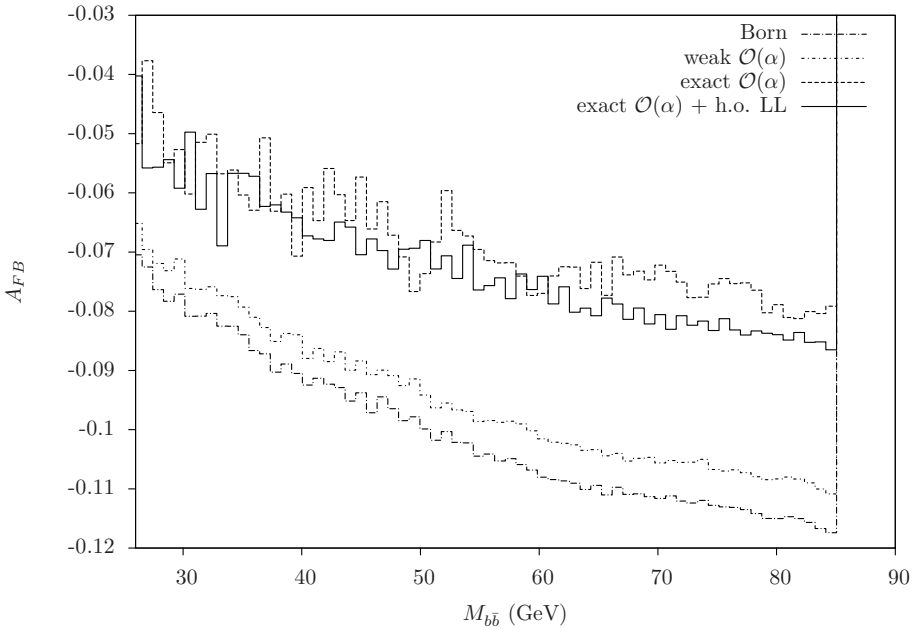

Figure 17: $A_{\rm FB}$ distribution at the Z peak.

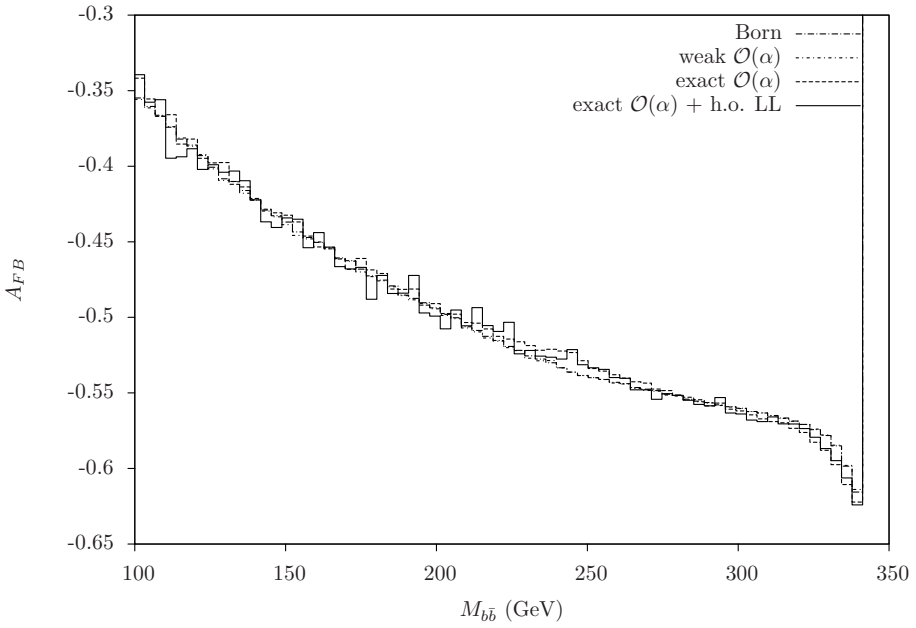

Figure 18: $A_{\rm FB}$ distribution at 350 GeV.

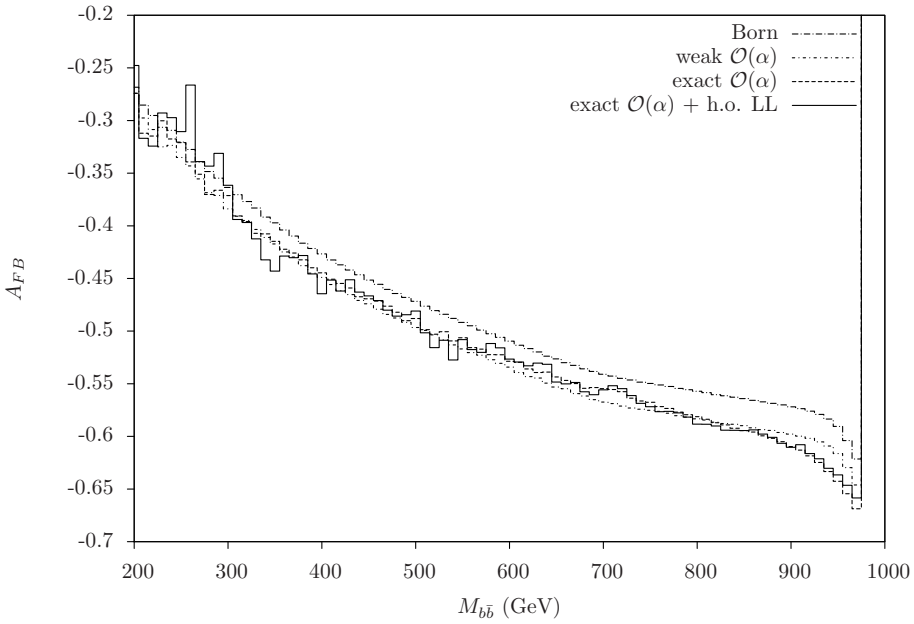

Figure 19: $A_{\rm FB}$ distribution at 1 TeV.

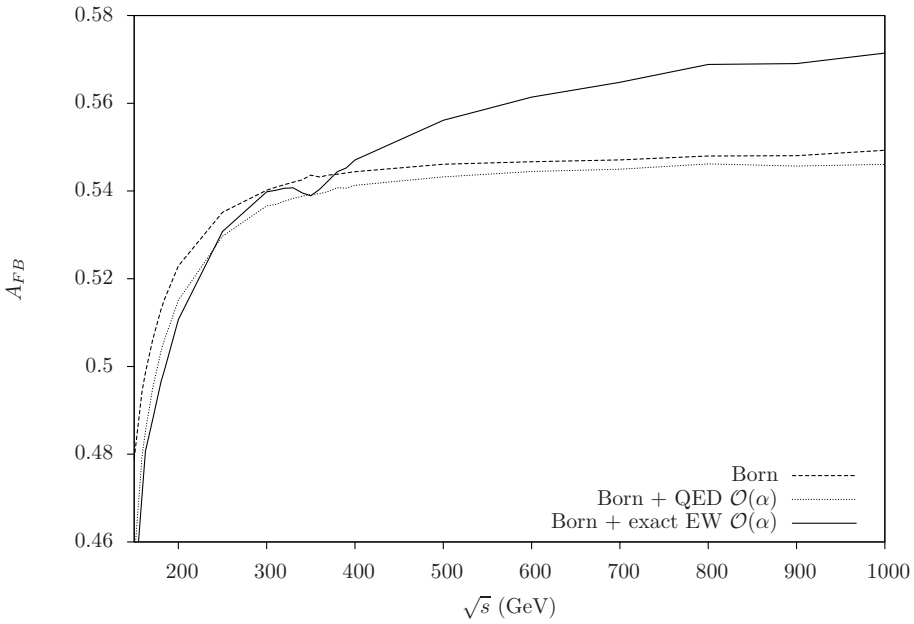

Figure 20: $A_{\rm FB}$ as a function of the CM energy, obtained at tree level, adding only QED corrections and the full one-loop EW corrections.

References

[1] S. Bethke, Eur. Phys. J. direct **C4** (2002) 1.

[2] A. Ballestrero, E. Maina and S. Moretti, Phys. Lett. **B294** (1992) 425; Nucl. Phys. **B415** (1994) 265.

[3] G. Rodrigo, A. Santamaria and M. Bilenky, Phys. Rev. Lett. **79** (1997) 193; J. Phys. **G25** (1999) 1593; hep-ph/9802359; G. Rodrigo, hep-ph/9703359; Nucl. Phys. Proc. Suppl. **54A** (1997) 60; W. Bernreuther, A. Brandenburg and P. Uwer, Phys. Rev. Lett. **79** (1997) 189; A. Brandenburg and P. Uwer, Nucl. Phys. **B515** (1998) 279; P. Nason and C. Oleari, Phys. Lett. **B407** (1997) 57; Nucl. Phys. **B521** (1998) 237.

[4] C. M. Carloni Calame, S. Moretti, F. Piccinini and D. A. Ross, arXiv:0804.3771 [hep-ph].

[5] C. M. Carloni Calame, S. Moretti, F. Piccinini and D. A. Ross, arXiv:0804.1657 [hep-ph], to appear in the proceedings of '8th International Symposium on Radiative Corrections (RADCOR 2007): Application of Quantum Field Theory to Phenomenology', Florence, Italy, 1-6 October 2007.

[6] E. Maina, S. Moretti, M. R. Nolten and D. A. Ross, hep-ph/0407150; hep-ph/0403269; JHEP **04** (2003) 056.

[7] Yu. L. Dokshitzer, G. D. Leder, S. Moretti and B. R. Webber, JHEP **08** (1997) 001; S. Moretti, L. Lönnblad and T. Sjöstrand, JHEP **08** (1998) 001.

[8] U. Baur, Phys. Rev. **D75** (2007) 013005.

[9] S. Moretti, M. R. Nolten and D. A. Ross, Phys. Rev. **D74** (2006) 097301; Phys. Lett. **B643** (2006) 86; Phys. Lett. **B639** (2006) 513 [Erratum, *ibidem* **B660** (2008) 607]; Nucl. Phys. **B759** (2006) 50; E. Maina, S. Moretti, M. R. Nolten and D. A. Ross, Phys. Lett. **B570** (2003) 205.

[10] See, e.g.: ALEPH Collaboration, 'QCD studies with e^+e^- annihilation data at 189 GeV', ALEPH 99-023, CONF 99-018, June 1999 (pPrepared for the International Europhysics Conference on High-Energy Physics (EPS-HEP 99), Tampere, Finland, 15-21 Jul 1999).

[11] S. Brandt, Ch. Peyrou, R. Sosnowski and A. Wroblewski, Phys. Lett. **B12** (1964) 57; E. Farhi, Phys. Rev. Lett. **39** (1977) 1587.

[12] R. K. Ellis, D. A. Ross and A. E. Terrano, Nucl. Phys. **B178** (1981) 421.

[13] See, e.g.: Z. Kunszt and P. Nason, (conveners), in proceedings of the workshop 'Z Physics at LEP1' (G. Altarelli, R. Kleiss and C. Verzegnassi, eds.), preprint CERN-89-08, 21 September 1989 (and references therein).

[14] See `http://lepewwg.web.cern.ch/LEPEWWG/`.

[15] See `http://www-sld.slac.stanford.edu/sldwww/sld.html`.